Korean J. of Chem. Eng., **12**(3), 273-276 (1995)

THE FALLING LAMINAR JET OF SEMI-DILUTE POLYMER SOLUTIONS

Jae Keun Lee† and Gyo Taeg Seo*

Research Center, Korea Electric Power Corporation, Taejon 305-380, Korea
*Department of Chemical Engineering, Chung Cheong College, Chung Buk 363-890, Korea
(Received 20 April 1994 • accepted 7 February 1995)

Abstract—The studies of falling laminar jets have been done mainly on Newtonian jet due to the complexity of non-Newtonian fluid parameter. Numerical solutions of the Newtonian jet equation are in good agreement with the experimental results of polymer solutions in the experimental concentration range. Numerical simulation results suggest that the free falling jet is mostly influenced by the Froude number. The jet radius increases with the Froude number. It was found that surface tension or viscosity does not contribute much to the shapes of the free falling jet.

Key words: *Laminar, Falling Jet, Newtonian, Non-Newtonian, Polymer Solution*

INTRODUCTION

A free falling laminar jet issuing from a circular nozzle under gravity is an important techique for the study of elongational viscosity and fiber spinning processes. The rheological expressions for the stress tensor of non-Newtonian fluids make formulation of the jet equation difficult. Therefore, the prediction of jet shapes at arbitrary flow conditions has been reported mainly on Newtonian fluid jets.

The first step in analyzing the fluid dynamics of a jet is the development of the shape equation of the jet diameter along the length. Scriven and Pigford [1957] proposed that in inviscid vertical jets, the velocity profile becomes nearly flat not too far downstream and the acting force is gravity. Therefore the velocity as a function of jet length, x, is given by

$$U=\sqrt{U_o^2+2gx} \tag{1}$$

and then from the continuity equation he derived the jet shape equation as

$$\frac{r}{R}=\sqrt[4]{\frac{x}{Fr \cdot R}+1} \tag{2}$$

Another shape equation for a free laminar jet initially in Poiseuille tube flow was developed by Lienhard [1968] using two dimensionnal boundary layer equations. Flow conditions are limited to $We \geq 100$ and $50 \leq Re \leq 1050$. The jet shape equation and the axial velocity are given as

$$\frac{r}{R}=\sqrt[4]{2\frac{Re \cdot x}{Fr}+\frac{16}{9}} \tag{3}$$

$$U=\sqrt{2\frac{Re \cdot x}{Fr}+\frac{16}{9}} \tag{4}$$

The equation of an inertial jet issuing from a vertical jet were derived by Anno [1977] from the Navier-Stokes equations for steady state. For an inviscid fluid it is assumed that the jet radius r(x) is not a strong function of jet length and U=U(x). The solution in terms of radius is

$$\frac{x}{Fr \cdot R}=\left(\frac{R}{r}\right)^4-1+\frac{4}{We}\left(\frac{R}{r}-1\right) \tag{5}$$

The governing equations of one dimensional flow of a viscous fluid have been developed by several researchers. The basic assumptions are that the jet is one dimensional and the axial velocity is flat across the jet. Pearson and Matovich [1969] derived the steady axisymmetric equation of a molten threadline considering viscous, inertia, gravity, and surface tension forces. The resulting momentum equation of a threadline in a Newtonian fluid is given by

$$\rho UU'=\rho g-\frac{3\eta U'^2}{U}+3\eta U''-\frac{\delta\sqrt{\pi U'}}{2\sqrt{QU}} \tag{6}$$

with boundary conditions $U(0)=U_o$ and $U(l)=U_1$, where the primes denote differentiation with respect to x. There is no analytical solution of this equation. Petrie [1979] introduced the force balance on an axisymmetric Newtonian jet element with the assumption that the jet is one dimensional and the air drag is negligible.

$$3\eta U'(x)A(x)=\int_x^l \rho gA(x)\partial x-2\pi\delta[R(x)-R(l)]-\rho Q[U(l)-U(x)] \tag{7}$$

Differentiation of Eq. (7) using $A(x)=Q/U(x)$ and $R(x)=\sqrt{A(x)/\pi}$ yields a second order nonlinear ordinary differential equation

$$3\eta\left(U''(x)-\frac{U'(x)}{U(x)}\right)^2=-\rho g+\frac{\delta}{2}\sqrt{\frac{\pi U'(x)}{QU(x)}}+\rho U(x)U'(x) \tag{8}$$

Cruickshank and Munson [1982] transformed Eq. (8) into a dimensionless form as follows.

$$FrUU'=1+\frac{3}{Re}\left(U''+\frac{U'^2}{U}\right)-\frac{Fr}{2We}\left(\frac{U'}{\sqrt{U}}\right) \tag{9}$$

where Fr, We, and Re are fomulated in a slightly different form. The velocity and inner radius at tube exit are used as the characteristic velocity and length parameter, and $Fr=U_o^2/gR_o$, $We=\rho R_oU_o^2/\delta$, and $Re=\rho R_oU_o/\eta$.

An important aspect of the analysis of liquid jets is the formula-

†To whom all correspondences should be addressed.

tion of appropriate boundary conditions for downstream from the jet nozzle. Dutta and Ryan [1982] proposed that the axial velocity is uniform at a distance where the jet length equals one nozzle diameter, and the radial velocity at the jet surface is zero. Vrentas et al. [1985] mentioned that Dutta's conditions are incorrect. By using those conditions the momentum equation for large distance from the nozzle becomes

$$\frac{\partial P}{\partial R}=0 \tag{10}$$

$$\frac{\partial P}{\partial x}=\rho g \tag{11}$$

These equations imply that the radially constant pressure in the jet increases linearly with x. However everywhere along the jet surface at sufficiently large downstream position the surface boundary condition becomes

$$P=0 \tag{12}$$

Therefore the pressure becomes zero everywhere at sufficiently large jet lengths from Eq. (10) and Eq. (12). This result is inconsistent with the linear pressure increase from Eq. (10) and Eq. (11). According to Adachi [1987], appropriate boundary conditions should be formulated at a distance not far downstream at a position where the velocity and the pressure are uniform over the cross section of a circular jet. An upper boundary condition depends on the flow emerging from the nozzle. From the continuity equation a possible lower boundary condition is

$$U=U_o\left(\frac{R_o}{R}\right)^2 \tag{13}$$

In general, it is impossible to introduce sufficiently detailed conditions on the velocity field at a finite length of a jet that is presumably of infinite length. Because of this, some jet studies were carried out in stagnation flow at a certain distance and often a take up speed is used for the lower boundary condition in the fiber spinning jet.

In this study, a comparison has been made between the experimental results of polymer solutions and the numerical results of Newtonian fluid. Cruickshank equation was used to analyze the effect of dimensionless parameter.

EXPERIMENT

Poly(ethylene oxide) (PEO) was chosen for study. The PEO was Polyox WSR-301 manufactured by Union Carbide Corporation. Weight average molecular weight is estimated to be 4×10^6. The poly(ethylene oxide) initially was wetted with 5 wt % of glycerin and then dissolved in distilled water to produce a stock solution concentration of 10,000 ppm by weight. These concentrated solutions were diluted to the final concentration and 20 liter diluted solutions were stored in polypropylene bottles at least a week to allow for homogeneous mixing before each run. The concentrations of test solutions were in the range 500 to 5000 ppm. The conductivity of the distilled water measured with a Barnstead Nanopure system was $1.7\times10^{-6}\,\Omega^{-1}\mathrm{cm}^{-1}$.

The jets were produced from the nozzle by gravity at 20℃. The nozzle had inside diameter 1.60 mm and length 1.0 cm. The jets were photographed. An aperture of f8 and a shutter speed 1/60 sec, a macro zoom lens, and lighting were used with Tmax 400 film. Measurements of diameter along the threadline were obtained from negatives projected on a white wall. The magnification factors (×15) of negatives without loss of sharpness were determined by comparing the outside diameter of the nozzle images with its known outside diameter. The flow rate was taken by measuring a volume of solutions leaving the nozzle in a given time with a graduated cylinder and a stopwatch. Surface tensions of solutions were measured by a capillary rise method. This method depends on the fact that the liquids will rise in a fine glass capillary tube only until the surface tension force just balances the force of gravity on the column of liquid. Densities of solutions were measured by weighing a known volume of fluid in a pycnometer using a Mettler balance. Viscosities of solutions were measured in a constant temperature bath at 20℃. Cannon-Fenske capillary viscometer were used.

MATHEMATICAL FORMULATION

The free falling jet equation used for the numerical approach is the Cruickshank equation in dimensionless form

$$\mathrm{Fr}UU'=1+\frac{3}{\mathrm{Re}}\left(U''+\frac{U'^2}{U}\right)-\frac{\mathrm{Fr}}{2\mathrm{We}}\left(\frac{U'}{\sqrt{U}}\right) \tag{9}$$

The basic assumption made in this equation is that the jet is one dimenensional and the axial velocity is constant across the jet. This second order nonlinear ordinary differential equation was solved by a finite difference method. Eq. (9) can be rewritten in the convenient form

$$\left(\mathrm{Fr}U-\frac{3}{\mathrm{Re}}\cdot\frac{U'}{U}+\frac{\mathrm{Fr}}{2\mathrm{We}}\cdot\frac{1}{\sqrt{U}}\right)U'-\frac{3}{\mathrm{Re}}\cdot U''=1 \tag{14}$$

If we discretize Eq. (14) using central differencing

$$\frac{\partial U}{\partial x}=\frac{U_{i+1}-U_{i-1}}{2\Delta x} \tag{15}$$

$$\frac{\partial^2 U}{\partial x^2}=\frac{U_{i+1}-2U_i+U_{i-1}}{\Delta x^2} \tag{16}$$

then Eq. (14) would be

$$\left[\mathrm{Fr}U_i^*-\frac{3}{\mathrm{Re}U_i^*}\left(\frac{U_{i+1}^*-U_{i-1}^*}{2\Delta x}\right)+\frac{\mathrm{Fr}}{2\mathrm{We}}\cdot\frac{1}{\sqrt{U_i^*}}\right]\left(\frac{U_{i+1}-U_{i-1}}{2\Delta x}\right) -\frac{3}{\mathrm{Re}}\left(\frac{U_{i+1}-2U_i+U_{i-1}}{\Delta x^2}\right)=1 \tag{17}$$

where * represents old values. Rearrangement of Eq. (17) results in triagonal system

$$\left(-\frac{A}{2\Delta x}-\frac{3}{\mathrm{Re}\Delta x^2}\right)U_{i-1}+\frac{6}{\mathrm{Re}}\cdot\frac{U_i}{\Delta x^2}+\left(\frac{A}{2\Delta x}-\frac{3}{\mathrm{Re}\Delta x^2}\right)U_{i+1}=1 \tag{18}$$

where $A=\mathrm{Fr}U-\frac{3}{\mathrm{Re}}\cdot\frac{U'}{U}+\frac{\mathrm{Fr}}{2\mathrm{We}}\cdot\frac{1}{\sqrt{U}}$.

The resulting tridiagonal system can be solved by subroutine TRIDAG.

RESULTS AND DISCUSSION

Comparison between experimental data and numerical values was made to see the usefulness of the Newtonian jet equation. Numerical values of jet radius using the Newtonian jet expression, Eq. (9), give reasonably good fits to the experimental data of 500 ppm, 1000 ppm, 3000 ppm, and 5000 ppm PEO solutions. These

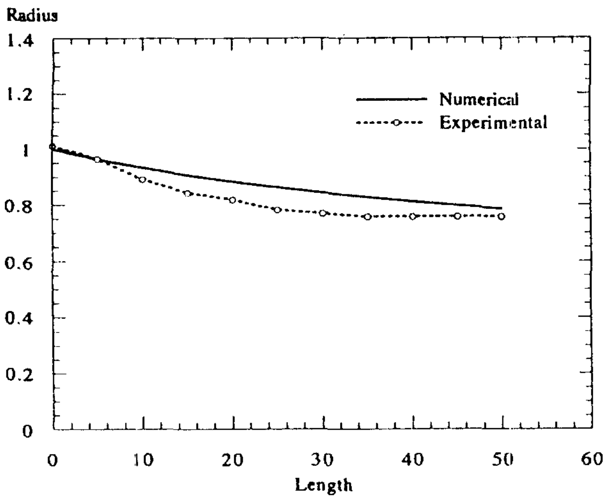

Fig. 1. Dimensionless radius vs. length for 500 ppm PEO jet. Fr #56.84, Re #348.48, We #4.89. The dashed line connects the data points.

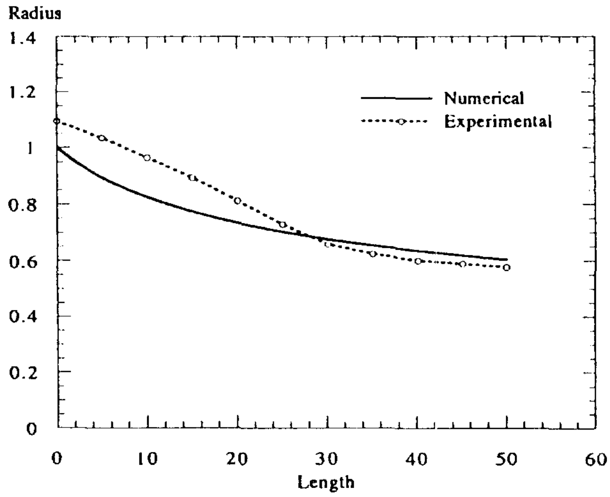

Fig. 3. Dimensionless radius vs. length for 3000 ppm PEO jet. Fr #12.92, Re #35.248, We #1.11. The dashed line connects the data points.

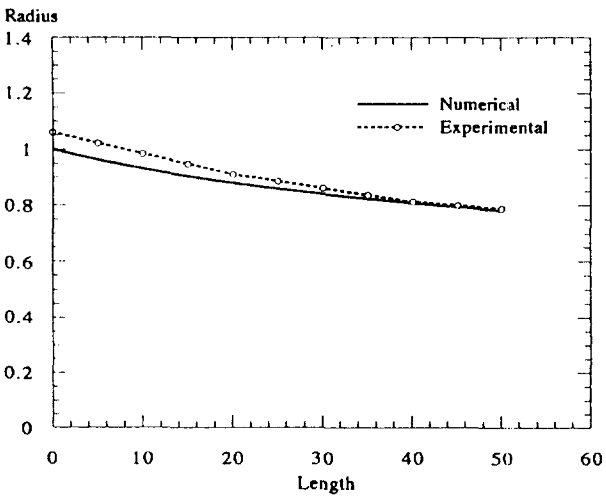

Fig. 2. Dimensionless radius vs. length for 1000 ppm PEO jet. Fr #55.11, Re #226.27, We #4.75. The dashed line connects the data points.

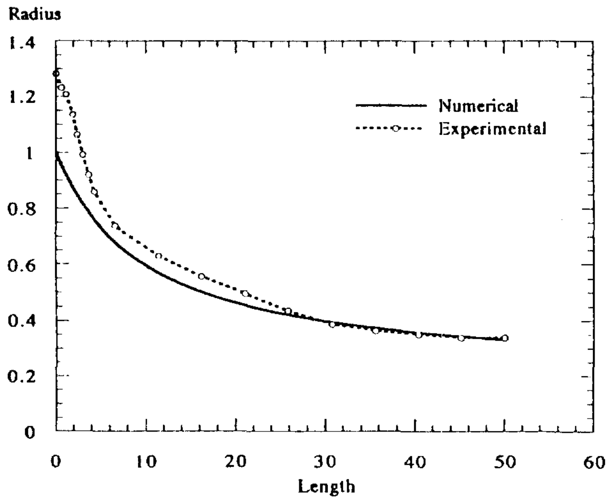

Fig. 4. Dimensionless radius vs. length for 5000 ppm PEO jet. Fr #0.645, Re #2.342, We #0.055. The dashed line connects the data points.

are shown in Fig. 1 through 4 in dimensionless form. Jet flow conditions are given in Table 1. In all cases the jet radius curves of numerical values approach the radius curves of the experimental values at a distance far from the tube exit. The spread between numerical values and experimental values of jet shapes near the tube exit is caused by the effect of jet swelling. The jet swelling ratio decreases as Reynolds number increases. It is thought that the Newtonian jet equation used here is useful as a reasonable approximation for semidilute polymer solutions. The free falling jet in our experimental range is expected not to produce an extensional flow field along the jet because there is no tensile stress to stretch the jet and the jet weight itself is not enough to produce the extensional flow.

The prediction of jet shape was made using a numerical approach over a wide range of flow conditions. At the same Reynolds number and Weber number conditions, the Froude number has an effect on the radius of the jet as shown in Fig. 5. The jet radius contraction follows the Froude number decrease. The effect of Weber number on jet shape at the same Froude number and Reynolds number is shown in Fig. 6. The Weber number increase causes a contraction of the jet radius. However, the effect of Weber number on jet shape is less profound, compared with the effect of Froude number. According to the results of Fig. 7, the Reynolds number by itself may not influence the shape of the radius. At three different flow conditions where Reynolds

Table 1. Jet flow conditions of PEO solution

Tube ID (mm)	Concentration (ppm)	U_0 ($cm \cdot sec^{-1}$)	ρ ($g \cdot cm^{-3}$)	δ ($dyne \cdot cm^{-1}$)	η (poise)
1.60	500	66.78	0.998	72.75	0.0153
	1000	65.75	0.998	72.75	0.0232
	3000	31.83	0.998	72.75	0.0721
	5000	7.11	0.998	72.75	0.2425

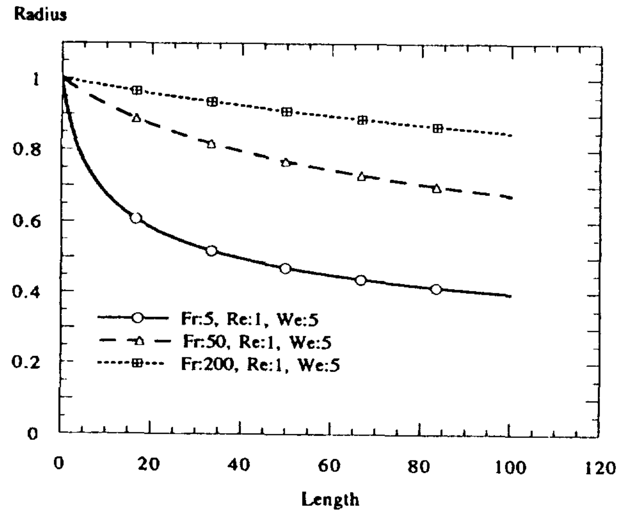

Fig. 5. Dimensionless radius vs. length as a function of Fr number. The lines represent the numerical values referring to Eq. (9).

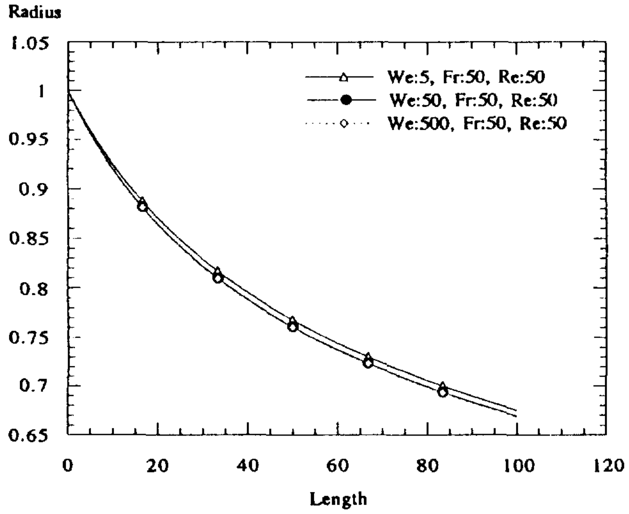

Fig. 6. Dimensionless radius vs. length as a function of We number. The lines represent the numerical values referring to Eq. (9).

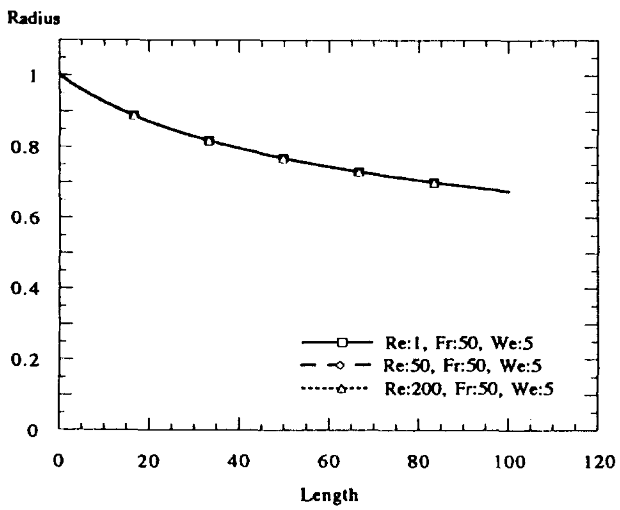

Fig. 7. Dimensionless radius vs. length as a function of Re number. The lines represent the numerical values referring to Eq. (9).

number is the only variant, the radius curves overlap. The most effective parameter is the Froude number, and the Weber number is the second effect, and Reynolds number the last.

CONCLUSIONS

When the jet is allowed to fall under gravity alone, the shape of the resulting jet of semidilute polymer solution was found to be suitable to Newtonian approximation because the jet weight itself does not induce enough tensile flow which is a characteristic of the polymer solution. The Froude number was the most important parameter in this analysis.

NOMENCLATURE

A(x)	: cross section at distance x [cm^2]
g	: acceleration of gravity [$cm \cdot sec^{-2}$]
P	: pressure [Pa]
Q	: volume flow rate [$cm^3 \cdot sec^{-1}$]
r	: jet radius [cm]
R	: nozzle inlet radius [cm]
R_o	: nozzle inlet radius at nozzle exit, characteristic length [cm]
U	: axial velocity [$cm \cdot sec^{-1}$]
U_o	: axial velocity at nozzle exit [$cm \cdot sec^{-1}$]
x	: jet length [cm]
ρ	: density [$g \cdot cm^{-3}$]
η	: shear viscosity [poise]
Fr	: Froude number, $\left(\frac{U_o^2}{2gR}\right)$ [-]
We	: Weber number, $\left(\frac{2\rho R U_o^2}{\delta}\right)$ [-]
Re	: Reynolds number, $\left(\frac{2\rho R U_o}{\eta}\right)$ [-]
δ	: surface tension [$dyne \cdot cm^{-1}$]

REFERENCES

Adachi, K., "Laminar Jets of a Plane Liquid Sheet Falling in the Atmosphere", *J. Non-Newt. Fluid Mech.*, **24**, 11 (1987).

Anno, J. N., "The Mechanics of Liquid Jets", Lexington Books, Lexington, 1977.

Cruickshank, J. O. and Munson, B. R., "The Viscous-Gravity Jet in Stagnation Flow", *Trans. ASME J. Fluids Eng.*, **104**, 360 (1982).

Dutta, A. and Ryan, M. E., "Dynamics of a Creeping Newtonian Jet with Gravity and Surface Tension", *AIChE J.*, **28**, 220 (1982).

Lienhard, J. H., "Effects of Gravity and Surface Tension upon Liquid Jets Leaving Poiseuille Tubes", *Trans. ASME J. Basic Eng.*, **90**, 262 (1968).

Pearson, J. R. A. and Matovich, M. A., "Spinning a Molten Threadline", *I&EC Fundam.*, **8**, 512 (1969).

Petrie, C. J. S., "Elongational Flows", Pitman, London, 1979.

Scriven, L. E. and Pigford, R. I., "Fluid Dynamics and Diffusion Calculations for Laminar Liquid Jets", *AIChE J.*, **5**, 397 (1957).

Vrentas, J. S., Vrentas, C. M. and Shirazi, A. F., "Downstream Boundary Conditions for Vertical Jets", *AIChE J.*, **31**, 1044 (1985).